The Plasma Magnet

NASA Institute for Advanced Concepts

# Phase I Final Report

John Slough

Department of Aeronautics and Astronautics

University of Washington

Seattle, WA 98105

Plasma Magnet: Sailing the Solar Wind

Two polyphase magnetic coils (stator) are used to drive steady ring currents in the local plasma (rotor) creating an expanding magnetized bubble. Expansion is halted by solar wind pressure is in balance with the magnetic pressure from the driven currents (R ≥ 10 km)
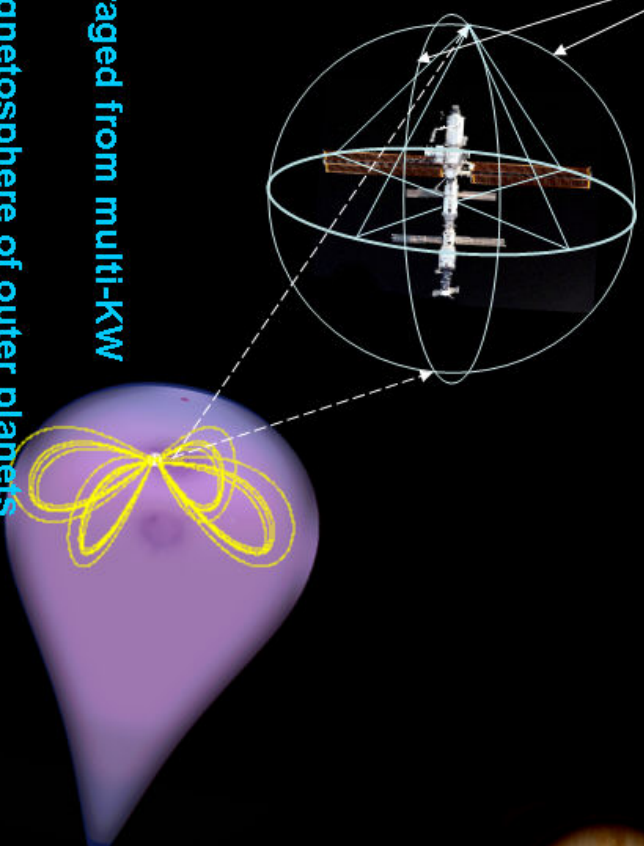
Applications:

- Multi-MW thruster leveraged from multi-KW RF power
- Magneto-braking in magnetosphere of outer planets
- Electrical power generation from back emf on RF field coils from solar plasma flow (solar windmill)
- Magnetic shielding of spacecraft from high energy solar particles

TABLE OF CONTENTS

Summary

Plasma sail propulsion based on the plasma magnet is a unique system that taps the ambient energy of the solar wind with minimal energy and mass requirements. The coupling to the solar wind is made through the generation of a large-scale ($\sim>$ 30 km) dipolar magnetic field. Unlike the original magnetic sail concept, the coil currents are conducted in a plasma rather than a superconducting coil. In this way the mass of the sail is reduced by orders of magnitude for the same thrust power. The plasma magnet consists of a pair of polyphase coils that produce a rotating magnetic field (RMF) that drives the necessary currents in the plasma to inflate and maintain the large-scale magnetic structure. The plasma magnet is deployed by the Lorentz self-force on the plasma currents, expanding outward in a disk-like shape until the expansion is halted by the solar wind pressure. It is virtually propellantless as the intercepted solar wind replenishes the small amount of plasma required to carry the magnet currents. Unlike a solid magnet or sail, the plasma magnet expands with falling solar wind pressure to provide constant thrust.

In phase I a small prototype plasma magnet was built and tested. The RMF coils generated over 10 kA of plasma currents with a radial expansion pressure sufficient to expand the dipole field to well over the 30 km scale that would supply as much as 5 MW of thrust power. The antenna and driver need weigh no more than 10 kg, and can operate from a 300 V supply. With the predicted scaling with size, it is possible to test the concept in the laboratory with a greatly enhanced laboratory solar wind source. Under phase II, a laboratory scaled experiment with an intensified solar wind source will assess the power gain predicted. With the successful demonstration of thrust power at the several hundred kW level, a final large tank test would be undertaken in phase III, and provide the final confirmation of the scaling for a space-based demonstration.

Background

It is highly unlikely that the higher speeds needed for outer planetary, manned planetary, or interstellar missions can be achieved from thrust provided by onboard power and propellant using conventional electric propulsion systems. Certainly, the power requirements are very much larger than can be supported by existing solar electric systems. With power requirements exceeding a few tens of kilowatts, the cost of any mission becomes prohibitive and access to deep space becomes very limited. There is certainly significant promise for any device that can generate megawatts of thrust power with minimal, kilowatt level, on-board power, and minimal fuel requirements. The plasma magnet has such potential. It would enable fast interplanetary scientific payload missions with very little development cost and in the near term. The physical principles involved in the plasma magnet current generation are well understood [2], and have been demonstrated in laboratory experiments [3].

There are several other possible uses for the plasma magnet besides propulsion. There is the less spectacular, but nonetheless important role as a magnetic shield for spacecraft from solar storms and high-energy particles, much as the earth's magnetosphere does. A plasma magnet generating magnetic dipoles within the earth's magnetosphere could be used for orbit raising and lowering depending on the direction and coupling to the Van Allen belts, and could thus be important for commercial satellite applications as well. But the singularly most important aspect of the plasma magnet is the possibility of achieving very high (multi-Megawatt) thrust powers, enabling manned interplanetary travel with only minimal resources, and no need for massive nuclear sources and shielding.

For the ambitious missions considered here it can be assumed that any near term mission must tap the energy available from the ambient medium. A possible alternate method is the deployment of a solar sail that would produce thrust on the spacecraft through the reflection and/or absorption of solar photons [4]. The solar sail presently consists of a thin film of aluminum with a polymer backing, providing a sail area of about 4000 to 15000 m^2, and would result in a net force of 25 to 75 mN. With present technology, the sail would have a mass density of about 20 gm/m^2 for a total weight of 80 to 300 kg.

Because of rapid developments in thin film technology, it is plausible to expect the mass density to drop by a factor of 2 to 4 in the near future. Nevertheless, it is seen that even with such reductions in weight the net thrust will not be substantially more than that for Deep Space 1. The main advantage of solar sails is that no propellant has to be expended, so that thrust can be maintained over extended periods. Larger sail areas are possible but problems associated with deployment have yet to be solved. There is, of course, no solution to the problem of a rapidly falling thrust as one moves out away from the sun.

The initial proposals to harness the energy of the solar wind were by reflection off a
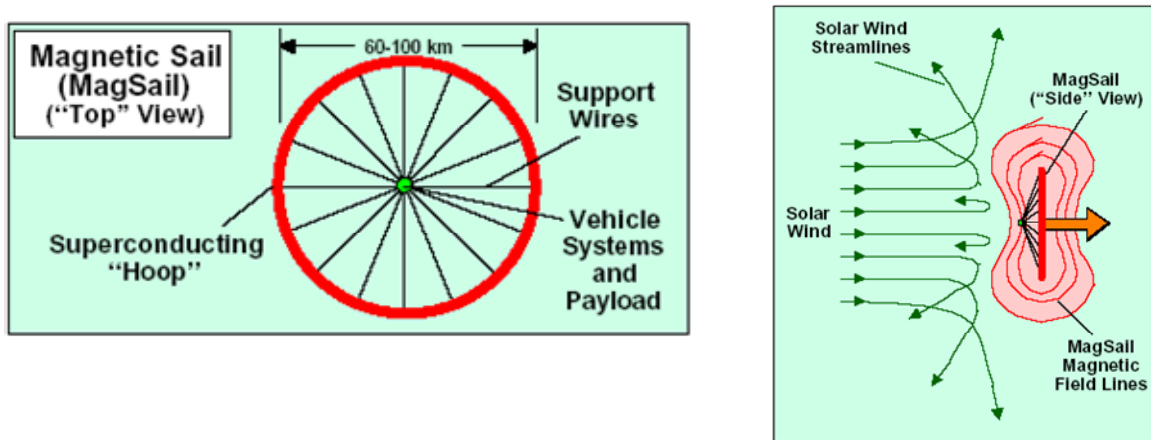
Figure 1. The Magnetic Sail (Zubrin and Andrews,1991).

magnetic wall or MagSail [5] (see Fig. 1). Here the basic concept was to deploy a huge superconducting magnet with a radius of ~ 30 km. A system of this size (~ a few metric tons) would only attain accelerations of the order of 0.01 m/s^2. The current density requirements for the superconducting ring are well beyond that of current high temperature superconductors, and again, there is that nagging problem of the thrust only being significant near the sun.

Mini-magnetospheric plasma propulsion (M2P2) is a novel propulsion scheme proposed by Robert Winglee [6]. The method makes use of the ambient energy of the solar wind by coupling to the solar wind through a large-scale (~ > 10 km) magnetic bubble or mini-magnetosphere. M2P2 is analogous to the solar and magnetic sails in that it seeks to harness ambient energy in the solar wind to provide thrust to the spacecraft. However, it represents

differences in several key areas. First, M2P2 utilizes electromagnetic processes (as opposed to mechanical structures) to produce the obstacle or sail. Thus, the technical and material problems that have beset existing sail proposals are removed from the problem.

In the initial embodiment of the plasma sail concept, the magnetosphere was to be inflated by the injection of plasma on to the magnetic field of a small (< 1 m) dipole coil tethered to the spacecraft. In collaboration with Prof. Winglee, an experiment, aimed at the demonstration of magnetic field inflation, was designed and constructed in collaboration with the proposer at the University of Washington (UW). In a further collaboration with the scientific staff at NASA Marshall Space Flight Center, the first prototype device was tested and demonstrated field expansion [7], albeit at a level that was below that desired for significant thrust in space, where a Newton of more of thrust (or a megawatt of thrust power) is desired.

The main difficulty with this approach to capturing the solar wind is the inflation of the relatively minuscule dipole field. The conditions required for inflation can be readily derived [8], but it can be seen that the magnetosphere must be inflated by plasma pressure, and the amount of expansion is directly proportional to the source plasma "beta" – the ratio of plasma energy to the local magnetic field energy, or $\beta = nkT/(B^2/2\mu_0)$. This makes for a significant challenge in that a local source of high β plasma will be difficult to sustain during initial inflation at magnetic fields high enough to generate a multi-kilometer size M2P2. The flux available to expand and interact with the solar wind is limited to that which can be generated in the small dipole coil. Although this flux can be expanded by a high β plasma, it can not be directly increased. It must be energized by the interaction with the solar wind, which cannot occur until the mini-magnetosphere is tens of kilometers in size. The thrust that can be developed by an M2P2 is thus ultimately limited by the magnetic flux of the on-board magnet in much the same way as the MagSail.

The plasma magnet has the advantages of the MagSail by directly maintaining a large scale magnetic structure, but by having the dipole currents carried not in a coil, but in a plasma, the large superconducting mass and shielding problems are avoided. Like M2P2, for a given amount of on-board power and fuel, the amount of thrust power that can be attained can be

several hundred times that of current propulsion systems, but without the size and power limitations imposed by a small dipole coil.

The ultimate spacecraft speed powered by the plasma magnet is that of the solar wind (350 to 800 km/s) which is orders of magnitude higher than the I_{sp} limitations of existing plasma thrusters. As opposed to the solar sails and the MagSail, the dynamic nature of the plasma magnet assures a constant thrust regardless of distance from the sun. The plasma magnet acts similar to a balloon (or magnetosphere) in that it will expand as the solar wind dynamic pressure decreases with distance from the sun. As such, it will provide a constant force surface and thereby provide almost constant acceleration to the spacecraft as it moves out into the solar system. The solar wind experiences essentially no deceleration until the termination shock at approximately 80 +/- 10 AU. The plasma magnet could thus be used for missions all the way to the Kuiper belt

In the initial embodiment for the plasma magnet, only solar electric systems are considered. This effectively limits the acceleration period to ~ 3 months (and the spacecraft speeds to 50 – 80 km/s). If larger electric systems become available that could provide a few tens of kilowatts of power, or if powered by either radioactive isotopes or nuclear power, speeds of several hundred km/s are possible.

The rotating magnetic field (RMF) that maintains the large-scale dipole currents can be constructed out of copper tubing, and driven by a simple oscillating tank circuit that operates at very high efficiency. Even though the plasma may be more resistive than the superconducting wires of the MagSail, the huge difference in cross sectional area that the plasma subtends (km^2 vs. cm^2) minimizes the additional power requirement. In recent experiments, a high power RMF system has operated at high efficiency (>90%) and at powers ~ 10 to 100 kW [9]. Given a viable way to erect an arbitrarily large-scale magnetic field together with the leverage of magnetospheric plasma propulsion, thrust powers of 10 to 100 MW should be achievable.

The most important aspect of the plasma magnet is the ability to **directly** drive the currents needed for the large-scale magnetosphere itself. Since the plasma electrons are magnetized in both the steady dipole field generated by the rotating magnetic field, as well as the RMF, the

plasma expansion effectively makes an ever-increasing plasma magnet, and ever increasing magnetic flux. The expansion, until halted by interaction with the solar wind, is essentially unstoppable. As plasma diffuses outward in the steady dipole, it is still driven by the rotating field and will still continue to generate a confining steady dipole field. In this way the plasma diffusion is countered by flux generation. In laboratory experiments conducted at the University of Washington (UW) [10], the plasma was confined for orders of magnitude longer than that predicted by classical Spitzer resistivity. It is quite possible that a plasma magnetic sail, driven and sustained by a rotating magnetic field, could be nearly propellantless as it traps the solar wind particles it intercepts which builds and sustains the magnetic field of the magnetosphere. The basic principles of how the plasma magnet works will now be discussed along with the key scaling requirements.

Analysis and Scaling of the Plasma Sail driven by a Rotating Magnetic Field

The plasma magnet generates the large scale currents needed for a large-scale magnetosphere by the entrainment of the plasma electrons in a rotating field created by two pair of loop antennae (see Fig. 2).
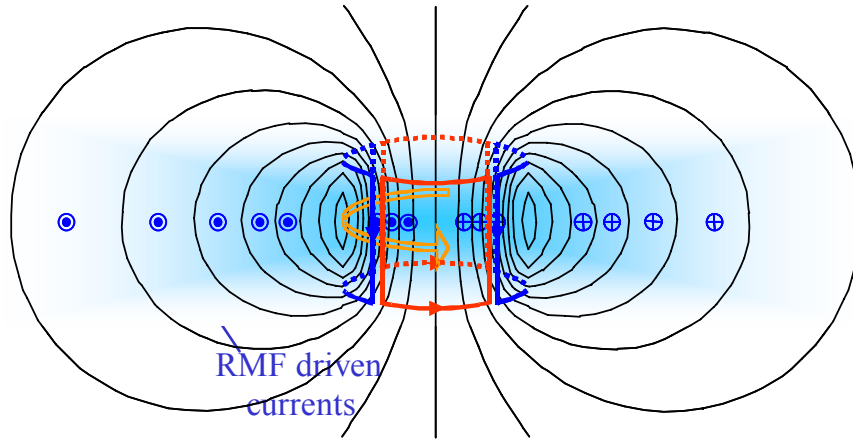

Figure 2. Plasma magnet configuration. The steady confining dipole field shown is produced by azimuthal currents driven in the plasma. The two pair of saddle coils (red and blue) carry RF currents that are phased to produce a magnetic dipole field that rotates in the equatorial plane (field not shown for clarity – see fig. 2).

To aid in perception, a cylindrical geometry will be assumed, where the steady dipole magnetic field has its axis in the z direction. Each pair of loop antenna are positioned opposite each other and carry an oscillating current which produces magnetic field whose axis lies in the equatorial plane. With the loop pairs separated by 90 degrees in azimuth, and with their respective currents separated in phase by 90 degrees, a steady magnetic field rotating in the equatorial plane is produced. In analogy to the induction motor, this is the same as the field that is produced in a two pole stator winding. Normally a "squirrel cage" rotor would be inserted inside these coils and the currents induced in the rotor by the rotating field, together with the stator magnetic field, produce the torque that causes the rotor to come into sychronous rotation with the field. Consider the case now where the metal rotor is replaced with a plasma rotor. With nearly zero mass, the electrons quickly come into co-rotation with the RMF. The

rigid rotation of the electrons is retarded slightly by collisions with the much more massive background ions which, due to their large inertia are unable to repond to the rapidly rotating field and remain motionless. In this manner a large azimuthal (θ) current is driven in the plasma. The magnetic field generated by the rotor currents couple it inextricably with the stator fields. Like any AC motor, a force appled to the rotor is reacted back on to the stator through these fields without any physical contact between the two. The same momentum transfer occurs with the plasma rotor as well. The eventual "load" on the plasma rotor will be the drag of the solar wind plasma, with the force of the solar wind reacted back onto the RMF antenna loops (the stator) attached to the spacecraft.

Currents driven by the RMF find an analogous representation in the ring currents formed when the magnetosphere is compressed by the solar wind (see Fig. 3). The process of course is reversed for the plasma magnet where the driven ring current acts to expand the magnetic
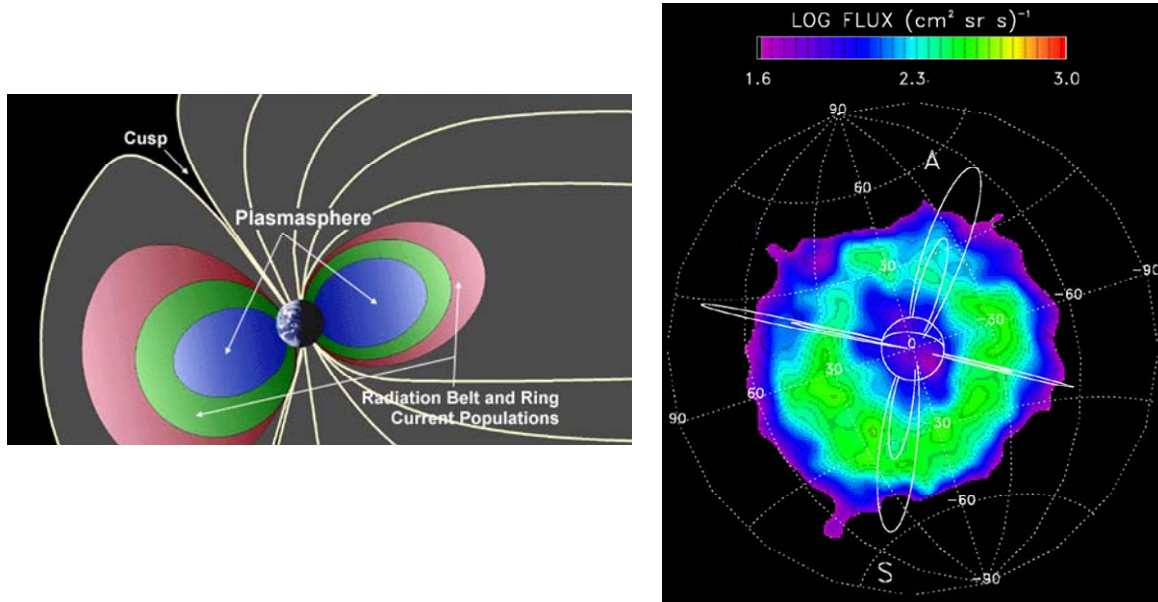

Figure 3. At left: Illustration showing the location of the ring currents in the earth's magnetosphere. At right: Image contours based on observation of the intensification of the ring current from compression in the solar wind.

bubble pushing off the solar wind.

For the plasma magnet to have a high efficiency, just as it is for the AC motor, there should be as little internal resistance as possible, i.e. the "no load" slip should be small. For the plasma this is the equivalent of satisfying two conditions: For there to be as large a current as possible, the ions should be unable to respond to the rotating field. This condition is met when the magnetic field is rotated faster than the ions can respond, or
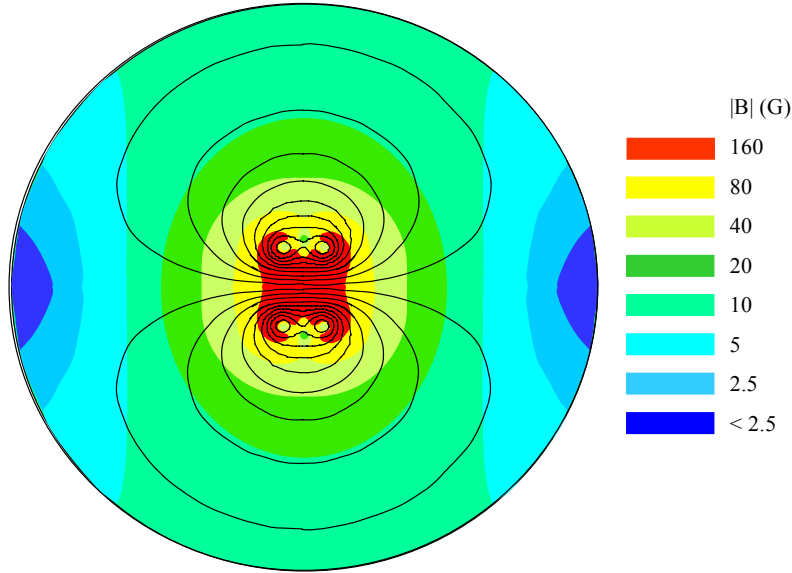

Figure 4. RMF lines and field magnitude in the equatorial plane from a pair of RMF antenna loops placed at a radius of 10 cm. The outer boundary at r= 0.5 m would be that of the stainless steel tank used in the experimental demonstration of the plasma magnet.

$$\omega_{RMF} > \omega_{ci} \tag{1a}$$

where ω_{ci} is the ion cyclotron frequency in the RMF. The slip du to the plasma resistivity is completetely analogous to the rotor slip in a motor due to resistive losses in the rotor. For the plasma rotor, the condition for a small slip is stated in terms of the plasma collisionality:

$$\nu_{ei} << \omega_{ce} \tag{1b}$$

where ω_{ce} is the electron gyrofrequency in the RMF. This inequality is equivalent to stating that the electrons are well magnetized to the RMF.

A starting point for understanding the current drive process is the generalized Ohm's Law, where it will be assumed for the moment that the ions form a fixed uniform background and the **u×B** term can be ignored [11]. The azimuthal (equatorial) current is determined by the θ component:

$$E_\theta + u_r B_z = \eta j_\theta + \frac{1}{ne}\langle j_z B_r \rangle = \eta\left[j_\theta + \left(\frac{\omega_{ce}}{\nu_{ei}}\right) j_z \right]$$ (2)

where B has oscillating components in the θ and r directions due to the RMF at a frequency ω_{RMF}, and a steady axial field B_z produced mainly by the RMF, but at least initially by a low field dipole coil. With a rotating field, the Hall term acting in the θ direction is comprised of a pondermotive component - the $\langle j_z B_r \rangle$ term. Since the axial screening current j_z and B_r vary similarly in time at the frequency ω_{RMF}, the pondermotive force in the θ direction has both a steady part and an oscillatory part at a frequency of $2\omega_{RMF}$. From the steady $\langle j_z B_r \rangle$ force, the electron fluid will attain that steady value of azimuthal velocity, $u_{e\theta}$ that corresponds to the balancing of the steady accelerating torque induced by E_θ, with the retarding torque due to the collisions of the electrons with the ions. In this way a steady azimuthal current density, j_θ is generated. For synchronous electrons, the azimuthal current density is given by:

$$j_\theta = -ne\omega_{RMF}r$$ (3)

where n(r) is the plasma density and r is the distance from the polar axis. This "rigid rotor" current density profile is characteristic of a low-slip RMF driven plasma. Operating the RMF antenna in the manner of the AC motor, very large (20 kA) currents have been generated in a plasma as small as 5 cm radius [9]. By having the azimuthal currents inside the RMF antenna, the expansion force of the current ring can be countered by an axial magnetic field produced by a coil surrounding the plasma just inside the RMF antenna. In this way an equilibrium can be established.

An additional requirement on the RMF is that it stay penetrated in the plasma. The solution of Ohm's law, neglecting the Hall term, is characterized by the RMF penetrating a distance $\delta = (2\eta/\omega\mu_o)^{1/2}$, which is the resistive skin depth for an RF field into a conductor. However, the

regime of interest here is a near collisionless plasma where $\nu_{ei} \ll \omega_{ce}$. In this limit, from Ohm's law, $j_\theta \approx -ner\omega$ and $j_z \approx E_z/(\eta\omega_{ce}^2/2\nu_{ei}^2)$. The electrons are in synchronous rotation with the RMF where their response to the axial electric field is severely restricted (small j_z), and unable to screen out the RMF. From another viewpoint, the co-rotating electrons experience a nearly steady transverse field, and the effective field penetration depth can be many times the resistive skin depth since the apparent frequency of the RMF in the frame of the electrons is near zero.

It should be recalled that RMF coils produce a dipole field that rotates in space with the dipole oriented with its axis in the equatorial plane of the steady dipole field. The discussion above has focused primarily on the current that can be generated by the synchronous rotation of the electrons on the inner dipole field of the RMF, since this is what has been extensively studied so far in the laboratory. To generate a large scale dipole magnet, one wants to flip the normal RMF current drive geometry inside out, with the plasma located in the region external to the RMF antennas as depicted in Fig. 2.

The larger picture of the RMF in the equatorial plane is shown in Fig. 4. From this figure, it can be seen that the outer field of the RMF dipole can be employed to drive azimuthal (equatorial) currents outside the dipole as long as there is plasma in this region.
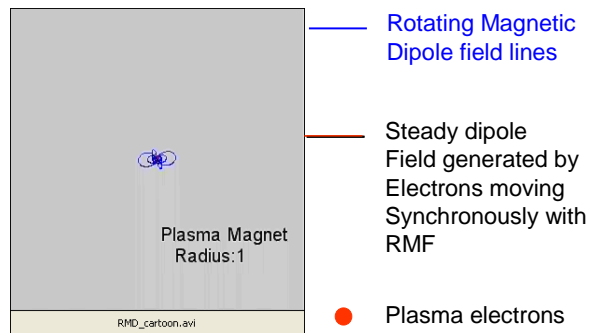
With no external field to oppose the Lorentz self-force acting on the plasma θ currents, the current ring expands. The only confining force is that of the curvature forces from the steady

dipole field created by the RMF driven currents. The movie clip above illustrates the principle of the generation and self-inflation of the Plasma Magnet.

This force is sufficient to keep the plasma in a high β equilibrium as it expands (the driven current is equivalent to a plasma diamagnetic current in equilibrium). Since the gyroradius of a solar wind ion will be much larger than the initially sub-kilometer size expanding dipole, little distortion of the dipole from the solar wind is expected until the plasma magnet has expanded large enough to interact with the solar wind. In addition to expanding the dipole, the driven currents will change the equilibrium field shape significantly from the vacuum field. Realistic equilibria for the magnetic dipole with large diamagnetic currents have recently been found and analyzed [12].

It was found that plasma pressure profiles $P(\psi)$ that fall off at least as slow as the adiabatic rate ($\sim \psi^{20/3}$), where ψ is the flux surface coordinate, were stable to both interchange and ballooning instabilities [13]. This is significant in that a well-confined plasma is important for maintaining a low plasma resistance as an anomalous plasma resistivity increases the amount of power that must be delivered to drive the same current. The modification to the dipole flux function ψ ($= \sin(\theta)^2/r$ in vacuum) at high β can be expressed as:

$$\beta \sim 0 \qquad \qquad \text{(dipole enlarged 10x)}$$
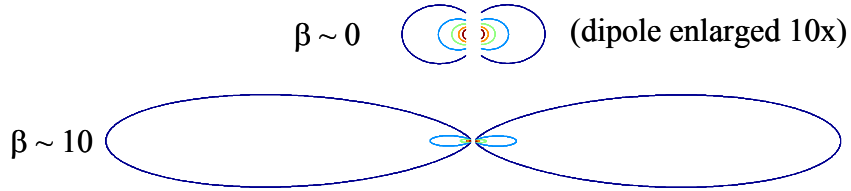
$$\beta \sim 10$$

Figure 5. Flux lines in R-Z plane for analytic equilibrium solution for a point dipole configuration at high β.

$$\psi = \psi_0 R_0^\alpha \frac{\sin(\theta)}{r^\alpha}, \quad \alpha = \beta_0^{-1/2},$$

where the zero subscript refers to a reference surface near the RMF antenna. As the current is increased, the flux function is considerably modified from the vacuum case as can be seen in Fig. 5. The flux surfaces become more disk-like as the plasma expands. This is primarily due

to the lower magnetic field of the dipole near the equatorial plane. As the plasma current (pressure) is raised, the dipole field is distorted into a shape that enhances the curvature force at the point of lowest field pressure (i.e. the equatorial region). In the limit of $\beta \to \infty$ (the plasma pressure equal to the external field pressure), the dipole field $B(r) \sim B_0 R_0^2 / r^2$.

With $\beta \gg 1$, the dipole field dropoff will at best no slower than $1/r^2$. This can be seen from from flux conservation. It is clear that the high β plasma will expand the flux over a much larger region (with equatorial area A). The initial dipole flux $\varphi_0 = B_0 A_0$ must equal BA at any point later. One has then that $B \propto 1/A \sim 1/r^2$. In addition, one must have good conductivity within the plasma (more accurately a sufficiently high magnetic Reynolds number) to keep the dipole flux from diffusing back to its original, unexpanded state. However, by directly driving the electrons in the outer magnetosphere, the plasma magnet grows with the expansion of the current ring. Diffusion is countered by an outward radial flow so that nothing can escape or impede the plasma from driving essentially as much current as Ohm's Law and the power supply will allow. The plasma is both created and ohmically heated by these RMF driven currents. Ohmic electron heating only helps to lower the plasma resistance making it even easier to drive a larger magnetosphere. The RMF current is driven in an inherently steady state manner, which allows for the continued expansion and sustainment of the configuration.

With the electrons magnetized to the RMF, the RMF is convected along with the dipole field as it expands and will thus also fall off as $1/r^2$. Since the solar wind compresses both the RMF as well as the steady magnetic dipole field produced by the RMF, it is reasonable to assume that the resultant field will fall off with the same r dependence $(1/r)$ as the dipole field did in the dynamically expanded magnetosphere calculations [6]. It is not necessary to make this assumption however. The RMF could drive the magnetosphere with the desired $1/r$ fall-off in the dipole field without the enhancement provided by the solar wind. This extra leverage assures that the magnetosphere produced by the plasma magnet will be of sufficient size regardless of the actual solar wind enhancement. The solar wind should only make it easier. To see how the $1/r$ dependence can be achieved by the plasma magnet alone, one determines the distribution of the RMF driven current density j_θ required to produce such a field. From Ampere's law:

16

$$j_\theta = \frac{1}{\mu_0} \frac{dB}{dr} = \frac{B_0 R_0}{\mu_0 r^2} \qquad (4)$$

Equating this expression with that for RMF current drive [Eq. (3)], it is observed that the plasma density can fall off as rapidly as $n \sim 1/r^3$, and still maintain the $1/r$ scaling for the dipole field. For a constant source production rate and no radial confinement (much like the solar wind), one has $n \sim 1/r^2$. Any plasma confinement, as well as any plasma introduced by the solar wind will provide an even slower density falloff. Driving more current than required for a $1/r$ is probably not a desirable condition, as the energy required to support such a high field increases dramatically for a field drop-off that is less than $1/r$. As the field expands then, the frequency of the RMF can be decreased proportionately to help maintain the j_θ scaling desired [see eq. (3)]. Reducing the RMF frequency would be required in any case for a very large plasma magnet, to keep the synchronous electrons from becoming relativistic.

During the initial expansion phase, the dipole will expand at roughly a constant rate so that $n \sim 1/r^2$. Without solar wind compression the electron cyclotron frequency will fall off with the RMF or, $\omega_{ce} \sim B_{RMF} \sim 1/r^2$. The electron-ion collision frequency, $\nu_{ei} \sim n \sim 1/r^2$, so that even with a decreasing frequency Eq. (2) remains satisfied. This dependence assures that if the RMF can drive the plasma near the antenna coils, it can drive a magnet of any radius as long as the $n \cdot \omega_{RMF}$ product falloff $\sim 1/r^3$ or better is maintained. A slower falloff however can most likely be sustained, since any heating of the magnetospheric plasma from the solar wind (and a large degree of heating is expected with compression) ν_{ei} will decrease as $T^{-3/2}$ as well.

The confinement of the plasma in the plasma magnet dipole field can be expressed as

$$\tau_N = \frac{\int n \cdot dvol}{4\pi r^2 D_\perp \frac{dn}{dr}} = \frac{2\mu_0}{3\eta_\perp \beta} \ln\left(\frac{r}{R}\right) r^2, \qquad (5)$$

where it has been assumed that the density decreases as $1/r^3$. (This is a conservative assumption as no confinement would lead to a $1/r^2$ scaling). With this assumption, the total plasma inventory N can be calculated as well with $N \sim 4\pi R^3 n_0 \ln(r/R)$. For an RMF antenna with R = 10 m with sufficient current (i.e. a particle density $n_0 \sim 10^{17}$ m^{-3}) to inflate to r = 100

km bubble, one has $\tau_N = 4.5\text{x}10^7$ s ~ 1.5 years! The total plasma mass for this bubble is $m_p \cdot N$ = 1.8 mg for hydrogen. Clearly refueling should not be a major concern for any working gas including Xenon.

The confinement of the plasma in the plasma magnet is a quantity that, most likely, will be determined empirically. In any case, once the expansion is complete, confining the plasma in a large scale plasma sail looks to be relatively easy. The simplest and most desirable method to achieve the desired density falloff is to simply reduce the particle flow from the source. If the confinement is good enough, or the entrainment of the solar wind sufficient, the source plasma fueling may be completely turned off.

If too great a density build-up should occur, it would be suppressed by the nature of the current drive process itself. As the density increases, the driven current increases, which increases the dipole magnetic field, and leads to a further expansion of the magnetosphere. The expansion drops the density, which reduces the current, and a new equilibrium is achieved. The expansion of the dipole is now only limited by the ohmic power needed to maintain the structure from resistive dissipation. To make a simple estimation of what this power would be, consider the case of an azimuthally uniform magnetic field where the 1/r dependence is found in all directions. This clearly represents the highest power loading, as this uniformly high field configuration demands the highest total current density (like a solar wind from all directions). The RMF power, P_{RMF}, needed to sustain the plasma magnet in this configuration is given by:

$$P_{RMF} = \int \eta j_\theta^2 \cdot dVol \quad \approx \quad \frac{\eta B_0^2 R_0^2}{\mu_0^2} \int_{R_0}^{R_M} \frac{4\pi}{r^2} dr$$

$$\cong \frac{4\pi\eta}{\mu_0^2} B_0^2 R_0$$

(6)

where eq. (4) was used for j_θ and B_0 represents the dipole field strength near the RMF coils. B_0 in eq. (6) can be restated in terms of the final expansion field and size based on the assumed 1/r field scaling:

$$B_0 = B_{MP} \frac{R_{MP}}{R_0}$$

(7)

Here B_{MP} is the magnetic field strength that is required to deflect the solar wind (i.e. the magnetopause field strength) and R_{MP} is the distance to the magnetopause along the Sun-magnetosphere line. For a solar wind density of 6×10^6 m^{-3} and a speed of $v_{sw} = 450$ km/s, the solar wind represents a dynamic pressure equal to 1 nPa. A magnetic field $B_{MP} = 50$ nT is sufficient to produce an equivalent magnetic pressure. One can ignore the solar magnetic pressure, as it is negligible compared to the supersonic plasma flow of the solar wind. From numerical calculations [6], it was found that the radial cross-sectional distance of the magnetosphere is roughly the same as the standoff distance R_{MP}. The thrust power from the solar wind intercepted by the magnetosphere is approximately:

$$P_{sw} = v_{sw} \cdot F_{MP} \sim v_{sw} \frac{B_{MP}^2}{2\mu_0} \cdot \pi R_{MP}^2 \qquad (8)$$

This expression is then solved with the above expressions for v_{sw} and B_{MP}. It can be restated in terms of P_{RMF} using eqs. (6) and (7) where it is conservatively assumed that the RMF power is half that found in eq. (6), since the solar wind is really only in one direction. The result is:

$$P_{sw} \sim \frac{\mu_0}{4\eta} v_{sw} R_0 P_{RMF} = 4.6 \times 10^3 R_0 P_{RMF} \qquad (9)$$

where Spitzer resistivity $\eta_\perp \sim 1.5 \times 10^{-3} T_e^{-3/2}$ with $T_e \sim 25$ eV was assumed. These values correspond to those that were observed in the STX experiments [10]. With the lower current and density requirements for the plasma magnet, a much higher T_e should be achievable. For example, in the larger but lower density experiments on STX [9], an electron temperature ~ 60 eV was observed. For the purposes of the scaling here, the more conservative estimate of the plasma resistivity will be used. The tremendous leverage in power one obtains from the plasma magnet can be easily seen from the numerical coefficient in eq. (9). With a 10 meter scale antenna and a conventional laboratory RMF power of 10 kW, a space based plasma magnet could produce a thrust power $P_{sw} \sim 460$ MW. Considerable inefficiencies can be tolerated before it would become disadvantageous to pursue this form of propulsion.

Since the gyroradius of a solar wind ion will be much larger than the sub-kilometer size expanding dipole, little interaction or distortion from the solar wind is expected during startup. The axisymmetric assumption then is likely to be quite valid until the plasma sail has reached a

size large enough for the solar wind to have a significant effect on it. Since it is sufficient for expansion that the driven currents be large enough for the field to fall off as r^{-2} (see eq. 4), this fall-off rate will be assumed. This corresponds to the case where the driven current in the plasma sail is just equal to the diamagnetic plasma current for a $\beta \gg 1$ dipole plasma. Besides expanding the dipole, these currents will change the equilibrium field shape significantly from the vacuum field. The flux surfaces become more disk-like as the β increases. This is primarily due to the lower magnetic field of the dipole as one approaches the equatorial plane. As the plasma pressure (current) is raised, the dipole field is distorted into a shape similar to that depicted in Fig. 3. Recalling that in the high β limit, the dipole field $B(r) \sim B_0 R_0^2 / r^2$, the total current in the dipole for a thin disk of radius R_{MP} can estimated from Ampere's law:

$$I_{tot} = \frac{1}{\mu_0} \oint B \cdot ds \quad \approx \quad 2 \frac{B_0}{\mu_0} \left[\frac{R_0^2}{r} \right]_{R_{MP}}^{R_0}$$

$$= \quad 2 \frac{B_0 R_0}{\mu_0} \tag{10}$$

for $R_{MP} \gg R_0$. The conditions required for the product of $B_0 R_0$ to achieve a magnetosphere with a magnetopause standoff distance, R_{MP} of 10 km, can be determined from eq. (6) above and is 5×10^{-4} T-m. For example, this could correspond to an initial field $B_0 = 50$ G, generated at the antenna radius $R_0 = 0.1$ m. The total current required in this case is $I_{tot} \sim 800$ A. If one were to not rely on the compression of the solar wind at all, the total current required in the plasma magnet to achieve the 1/r falloff would be,

$$I_{1/r} = \frac{1}{\mu_0} \oint B \cdot ds \approx 2 \frac{B_0 R_0}{\mu_0} \ln[r]_{R_M}^{R_0} = 9 \text{ kA} . \tag{11}$$

So even in the extreme case where all of the plasma currents are generated by the RMF, the total driven current is less than what has been achieved in the recent plasma magnet experiments during phase I.

The tremendous leverage in power one obtains from a RMF driven magnetosphere can be easily seen from the numerical coefficient in eq. (9). It is also noteworthy to realize how

relatively little energy must be invested in the plasma and field to produce a plasma sail of 10s of km dimensions.   The magnetic energy within the plasma sail is given by:

$$E_B \sim \int_{R_0}^{R_{MP}} \frac{B_0^2 R_0^2}{2\mu_0 r^2} \cdot 4\pi r^2 dr \quad = \quad \frac{\pi}{2\mu_0} B_0^2 R_0^2 R_{MP} \quad = \quad \frac{\pi}{2\mu_0} B_{MP}^2 R_{MP}^3 \qquad (12)$$

where the slower falloff of B under solar wind compression (B $\sim$ $B_0 R_0/r$) has been assumed. At a sail size of 30 km, and recalling that solar wind pressure corresponds to a field pressure, $B_{MP} \sim$ 50 nT, the total magnetic energy is only 84 kJ. A car battery stores 1 MJ.

  The details of the device that was built and how it operated will now be given.

Experimental Results

During phase I, a test of the basic principle of the plasma magnet was undertaken. Clearly, the most important objective was to demonstrate that a plasma magnet can be constructed that could produce and maintain the magnetic field required for the large-scale dipole, and this was accomplished successfully.   In addition, several other aspects of the concept were also demonstrated. The most significant results can be summarized as follows:

1. **A plasma magnet was generated and sustained in a space-like environment with a rotating magnetic field**
2. **Sufficient current (> 10 kA) was produced for inflation of plasma to 10s of km.**
3. **The plasma magnet intercepted significant momentum pressure from an external plasma source without loss of equilibrium**
4. **Plasma and magnetic pressure forces were observed to be reacted on to rotating field coils through electromagnetic interaction.**

An outline of the experimental setup as well as details of how each result was obtained will now be given.

The testing of the plasma magnet in a laboratory setting represented a unique challenge. Even in a large vacuum tank, the generation of the plasma magnetic dipole currents would cause a rapid expansion into the vacuum wall without a restoring force. To measure the performance of the device it was necessary to supply a confining pressure much like the solar wind will provide in space. Creating a plasma source that could produce this pressure was beyond the scope of a phase I study, but will certainly be the next step now that the proof of principle experiment has been realized. The confining pressure in the phase I experiments was supplied by a low field, large-scale external magnetic field perpendicular to the direction of expansion in the region of expansion.

As has been noted, a major attraction of the plasma magnet over other propellantless systems such as the original MagSail or solar sails is the dynamic expansion of the magnet as the spacecraft moves away from the sun and solar wind pressure drops. The converse of course should also be true. By taking advantage of this scaling, it is possible to test the plasma

magnet at full current and power in the small-scale laboratory experiment. This is accomplished by applying a sufficiently large external confining field. If the magnetic field is parallel to the polar axis, it will exert a radially inward pressure opposing the plasma expansion. The plasma magnet can thus be compressed to the meter scale from the kilometer as illustrated in Fig. 6.
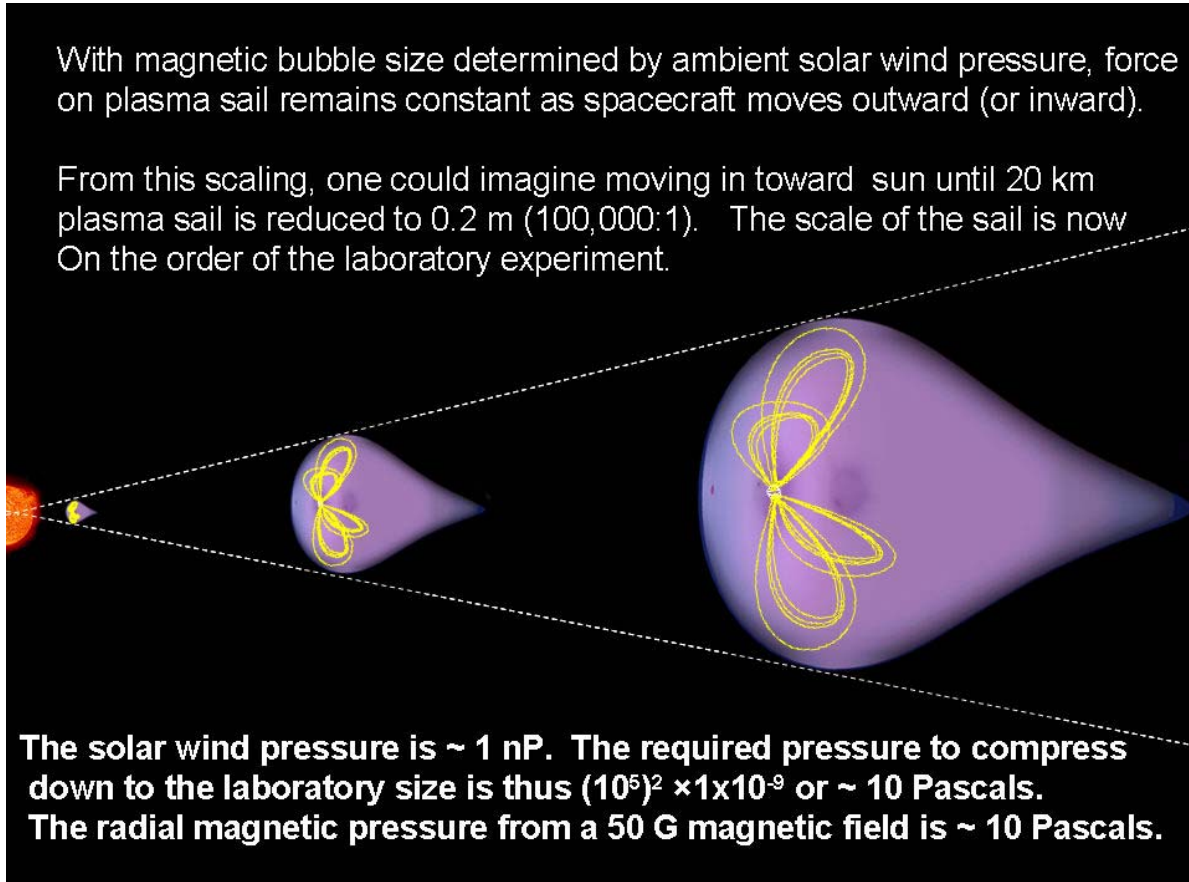

With magnetic bubble size determined by ambient solar wind pressure, force on plasma sail remains constant as spacecraft moves outward (or inward).

From this scaling, one could imagine moving in toward sun until 20 km plasma sail is reduced to 0.2 m (100,000:1). The scale of the sail is now On the order of the laboratory experiment.

The solar wind pressure is ~ 1 nP. The required pressure to compress down to the laboratory size is thus $(10^5)^2 \times 1 \times 10^{-9}$ or ~ 10 Pascals. The radial magnetic pressure from a 50 G magnetic field is ~ 10 Pascals.

Figure 6.

Given the ~ 1 meter diameter of the test chamber at the UW, a plasma magnet radius $R_M = 0.25$ m was chosen (see Fig. 7). Given the target radius desired in space of R_{MP}~ 30 km, the compression ratio of the laboratory test over the actual solar wind is ~ 10^5. Since the magnetic pressure scales as B^2, and $B \sim 1/r$ under compression, one has that the external field coils must produce a pressure that is 10^{10} larger than that of the actual solar wind pressure in order to

achieve the desired compression. As large as this factor may seem, it is in fact quite feasible, since the solar wind pressure is roughly 1 nPa at 1 AU.

The field pressure that corresponds to 10 Pa is ~ 5 mT (50 G).   The external tank Helmholtz coils on the vacuum chamber (red bands in fig. 4) produced an axial field of 100 G. It was possible experimentally to generate sufficiently strong plasma current to stand-off even this larger field. The equivalent expansion of this plasma would result in a plasma sail 4 times larger than the nominal 30 km. The device that was built during phase I had a RMF coils that
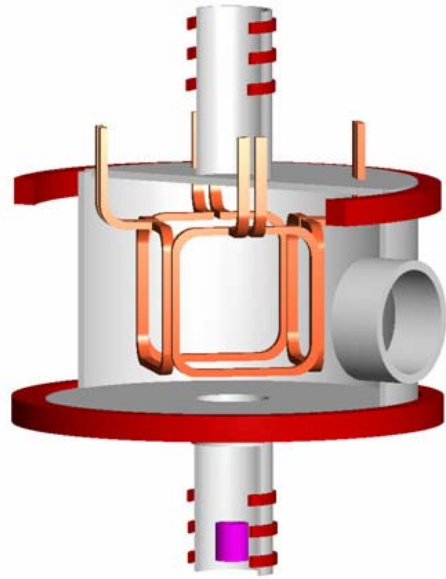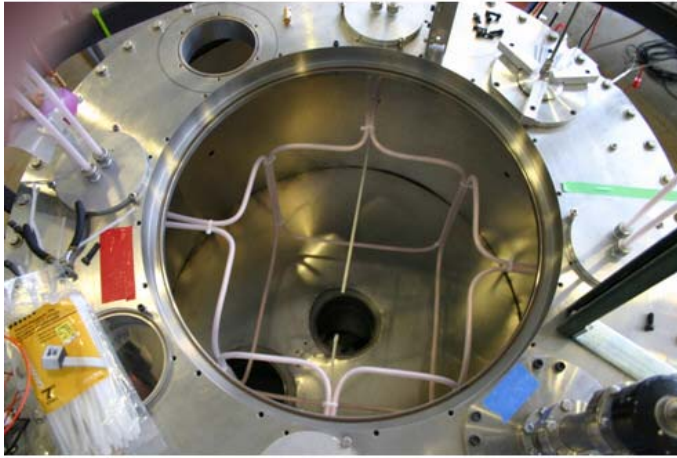

Figure 7.   Metal vacuum chamber with two pair of RMF coil sets for producing the B_x and B_y component of the rotating field.

were square shaped with mean radius of ~ 0.25 m. The shape is not critical and was chosen to fit conveniently into the available vacuum tank, and still leave plenty of room to observe current drive. (The cylindrical chamber had a diameter of roughly 1 m, and a height of 0.6 m). From eq. (9), it is clear that for a given available power, P_{RMF}, that the larger the antenna, the greater the intercepted solar wind power. The multiplier is essentially the leverage achieved over conventional propulsion. The electrical efficiency of an electric thruster is always less than unity and typically 0.6 or so. Here the power into the plasma is actually more efficiently coupled than in an electric thruster. There are ionization losses, but there is no thruster wall or frozen flow losses. Any power dissipated in the plasma from the RMF goes directly into heating the plasma, raising its β and producing a larger plasma current. Of course the huge multiplier makes this efficiency completely inconsequential.   In the experiment however a significant power flow from the RMF system must be maintained into the plasma due to boundary losses at this small scale. This is a consequence of the r^2 scaling in eq. (5). This power conveniently comes from the greater ohmic dissipation in the much higher current
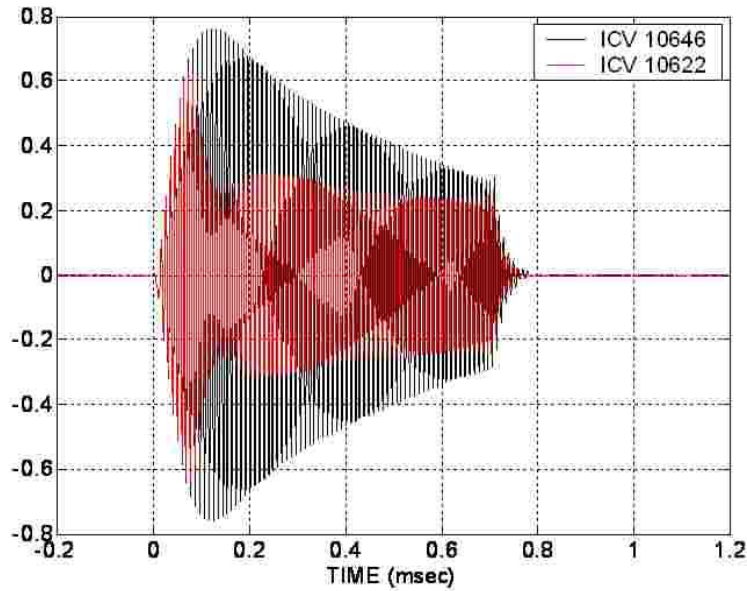

Figure 8.   Current waveforms (in kA) from an RMF coil in vacuum (black), and with plasma (red). The overall decay in the waveforms is due to limitation in power supply capacitive energy storage

density plasma in the laboratory plasma magnet. This high current density is due to the much greater compression required to keep the plasma magnet condensed to the meter scale. The power requirement will fall naturally as the scale increases, and this is what is essentially behind the size scaling in eq. (9).

The global resistance, and thus power needed to drive the plasma currents, is easy to measure experimentally as it can be determined from the increase in antenna loading observed during current drive compared to that in vacuum. Antenna current waveforms with and without plasma are shown in Fig. 8. For both this device as tested in the laboratory, and the future phase II tests, the RMF power required is on the order of 50-100 kW for sustainment. Only when a much larger chamber (~ 10 m scale) test is performed will the power required for sustainment begin to drop. Based on eq. (5), for a factor of 10 larger antenna than used here, one should need only $1/100^{th}$ the power for sustainment against plasma loss.

Figure 9. Setup for the RMF experiments at the UW.

The methodology for how to drive plasma currents has been worked out in previous experiments [15]. In these experiments, however, the desire was to drive current only in the inner region of an axial dipole coil. This allowed the RMF antennas to reside outside the vacuum vessel. The currents that need to be driven for a plasma sail are on the outside of the RMF antennas as well. The main challenge therefore for the phase I testing was to figure out the best way in which to build the RMF coils in a vacuum setting. It was decided for simplicity of the prototype, to leave the drive electronics outside the vacuum, and to pipe all the current feeds to the coils that would be positioned at the center of the stainless steel, cylindrical chamber (see Fig. 6). As can be seen in Fig. 6, the RMF is generated with two sets of two current loops.

Each current loop pair is composed of two loops that are positioned to form roughly a quasi-Hemholtz pair transverse to that of the steady axial Helmholtz field. The RMF antenna was made from No. 4 copper wire insulated by 3/8" OD polyethylene tubing. Each antenna pair was connected in series with a total inductance of 4 µH. These were placed in series with two paralleled 0.25 µF capacitors to form a series oscillator with a resonant frequency of 108 kHz. A pair of solid-state drivers and tuning circuits developed for RMF current drive experiments up to 100 kW power transfer is shown in Fig. 9.
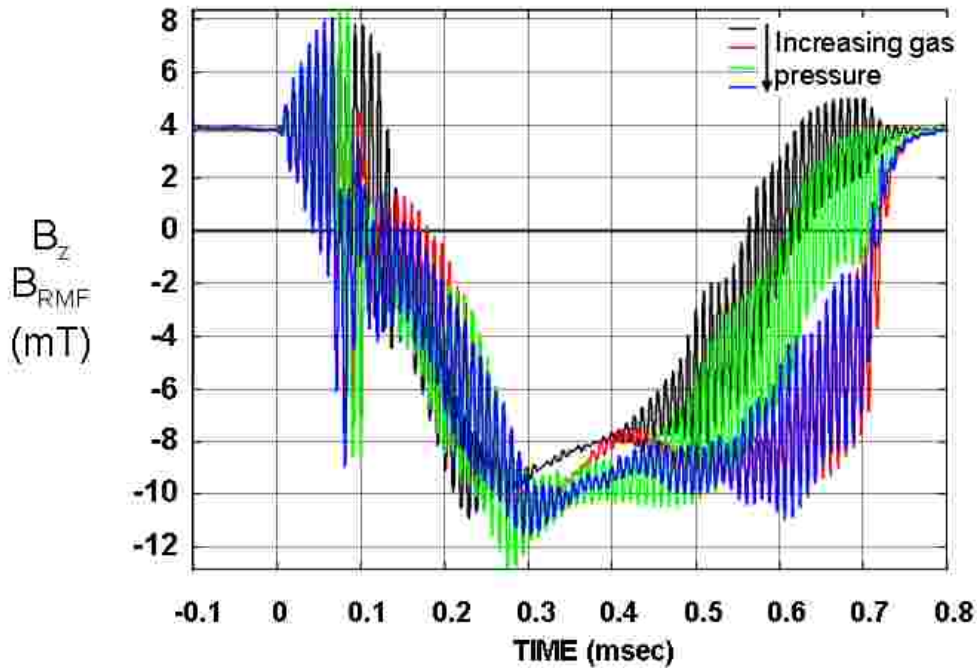

Figure 10. Time history of magnetic field on axis from RMF driven currents.

The unloaded (no plasma) antenna system (series driven L-C resonant tank) was found to have a reasonably high "Q" ($\omega L/R_{circuit}$) ~ 40. From an efficiency point of view it is a highly desirable condition to have a higher efficiency, and Qs as high as 300 have been achieved in the laboratory. The plasma loading drops the Q to as low as 15. This means that the power lost to the antenna circuit can be as small as 5% of the total power delivered to the antenna. In light of the prior discussion, achieving a high Q is of minor importance other than making plasma breakdown and power measurements easier.

While the prototype plasma magnet system was outfitted with several diagnostics. The bottom-line measurements of the plasma behavior and driven current were by far the most important. The azimuthal current driven by the RMF was obtained from the measured magnetic field profile inside the chamber from internal B-dot probes. By monitoring the field on the axis, a measure of the total current can be obtained from the magnitude of the axial magnetic field produced by the currents in the plasma magnet - just as it would be for any magnet. The magnetic waveforms for several discharges are overlayed in Fig. 10. The RMF was turned on for 0.7 msec. This was sufficient time to achieve pressure balance and equilibrium with the external Helmholtz field pressure (~ a few μsec). Longer pulses were not possible due to power supply limitations, but a steady plasma magnet equilibrium field of ~ 100 G was achieved. The field swings from positive to negative as the currents driven by RMF act to oppose the external Helmholtz field. The axial magnetic field radially outside of the plasma magnet was increased by the driven currents up to 80 G from the vacuum field value of 40 G, due to the flux conserving nature of the metal chamber wall. Due to the conducting wall, it was not possible for the plasma magnet to expand much beyond the 0.2 m it was observed to reach. The compression of the field trapped between the plasma and the wall prevented further expansion. A dielectric chamber is planned for phase II to avoid this problem. The magnetic probe traces in Fig. 7 were obtained with a multi-turn magnetic loop probe tilted at an angle of 45° to equatorial plane. This was done to measure simultaneously both the high frequency RMF as well as the steady axial field generated with roughly the same sensitivity. It can be seen that the magnitude of the RMF field is quite variable, but always present. This is due to the varying torque exerted by the RMF on the plasma electrons. Initially the RMF field is large (before significant plasma production). The plasma is rapidly ionized by the ohmically heated plasma from the rapidly rising azimuthal currents. The RMF amplitude decreases due to circuit loading and decay (see Fig.5), further decreasing the amplitude of the RMF field. Eventually the RMF field amplitude is restored as an equilibrium is established. The presence of the RMF ensures that plasma is magnetized to the RMF fields and the motion of the electrons is synchronous with this field.

The axial field passes through zero as one goes from inside to outside of the plasma magnet, as it does in a conventional magnet), but here the pressure forces are sustained by the plasma pressure, with the local plasma pressure equal to that of the external field pressure. The equilibrium plasma is thus by definition high β, and would rapidly expand if not confined by the compressed Helmholtz field.
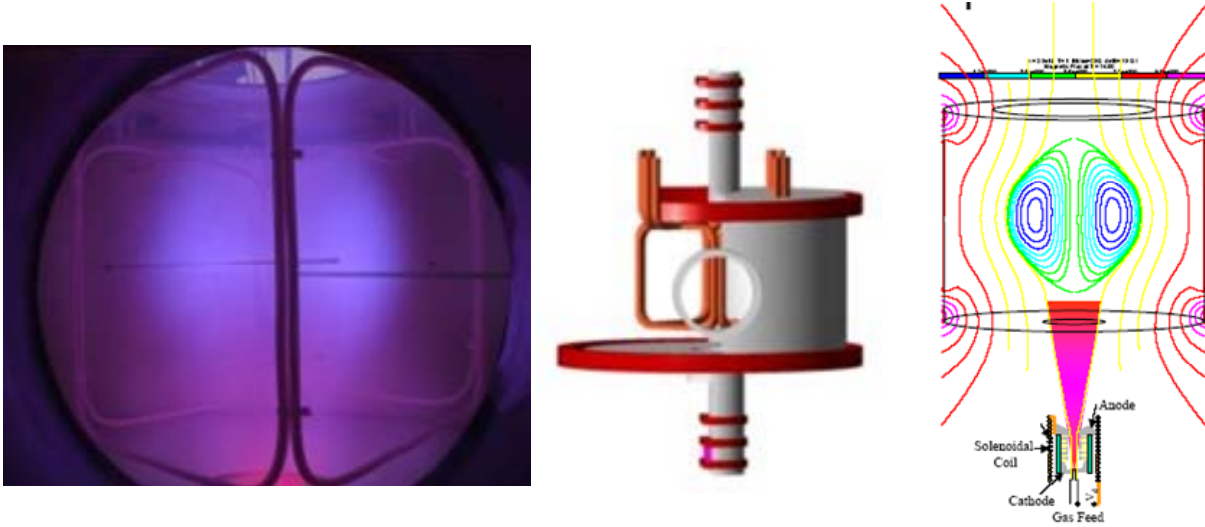

Figure 11. At left is a time integrated image of the plasma emission during an Argon RMF discharge. The center picture provides the perspective for the image. The figure at right is the 2D MHD equilibrium flux contours corresponding to the discharge conditions determined by the magnetic probe and Langmuir probe profiles, as well as external magnetic measurements.

A very useful diagnostic was a high resolution digital camera synchronized to the discharge. A large side-viewing port allowed, for the first time, the imaging of the high β plasma torus formed by the RMF. A time integrated picture of the plasma magnet is shown in Fig. 11. There are several noteworthy features to be mentioned. From the picture it is clear that the plasma magnet is distinct from the RMF antenna structure with no significant plasma contact. From spectroscopic measurements on the plasma light, the emission from the plasmoid is from Ar II emission lines, and not from neutral gas excitation or impurity light (see Fig. 12). The utter lack of Ar I lines in the time integrated spectra indicates a very rapid and complete ionization of the Argon gas. Since there is no flow of Argon gas into the chamber during the discharge this is not unexpected. Recombination is also minimal. This is due to the high electron temperature observed from Langmuir probe measurements where T_e was found

to be 18 eV. A similar temperature for the ions is inferred from pressure balance with the external Helmholtz field. All of these results were consistent with the 2D MHD equilibrium calculations that were made based on the measured magnetic and density measurements in the equatorial plane. A plot of the equilibrium flux contours are displayed in Fig. 11. From these
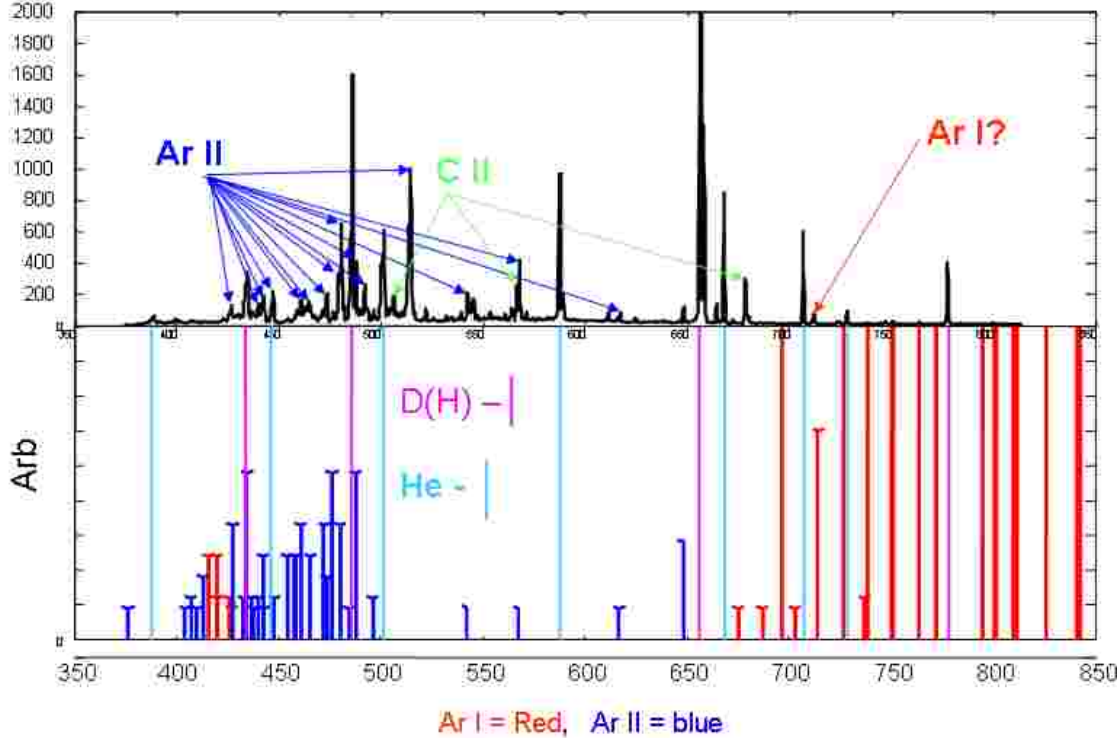

Figure 12. Time integrated visible spectra for a discharge in Argon. Reference linesand relative magnitudes shown in lower figure are from the NIST database.

calculations the total driven current is easily obtained and was found to greater than 10 kA for the discharge shown. Currents as high as 20 kA have been obtained at higher RMF power. Again, since the total current (or equivalently the final plasma sail size) is a function of antenna size (see eqs. 9 & 11), it makes far greater sense to make the antenna larger than drive a smaller antenna at high power, particularly given the low mass required for the antenna (10s of kg at most for a 10 m antenna). For near term experiments in smaller chambers, however, this is the only choice.

The preionization was provided by what is referred to as a Magnetized Cascaded Arc Source (MCAS) [16]. The effect of the plasma source on the plasma magnet will be discussed

31

directly, but suffice it to say, it is a copious plasma producer. A diagram of the device and measurements of the plasma production from the MCAS is given in Fig. 13. The gas used in the MCAS for these experiments was D_2 deuterium (accounting for the D(H) lines in the spectra in Fig. 12 as well as the magenta glow in the bottom of the picture in Fig. 11). The location of the MCAS (see Figs. 6 and 11) was chosen as far from the main chamber as possible. The reason for this was to avoid the jet-like supersonic plasma from possibly disturbing the formation of the plasma magnet. Initially, the use of the MCAS was primarily as a plasma initiator, to be turned off at the start of current build-up. It found however to be
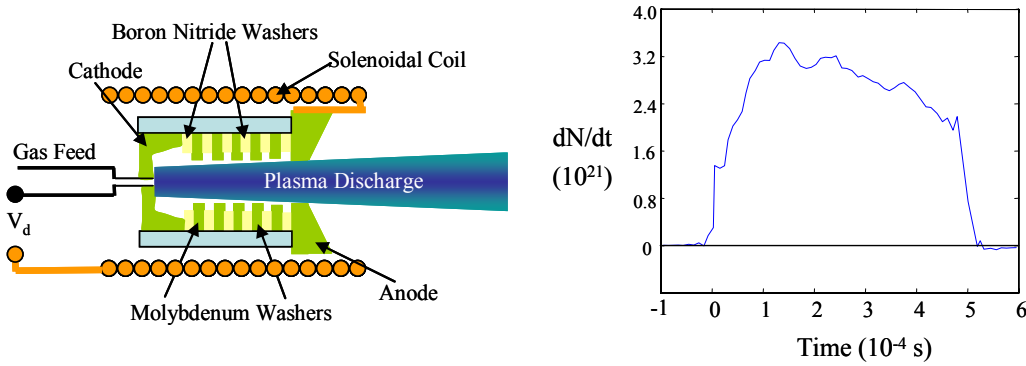

Figure 13. Schematic of the Magnetized Cascaded Arc Source, and a plot of the measured deuterium plasma output.

quite useful as an important test for the plasma magnet concept itself. By leaving the MCAS plasma jet on during the sustainment phase of the plasma magnet, a considerable force was applied at the lower end of the plasmoid from the plasma gun (see Fig. 11). This force would act to translate the plasmoid up into the quartz window at the top of the vacuum chamber if were not magnetically linked to the RMF antennas It is well known from previous studies that such a plasmoid is neutrally stable to translation and is readily translated with any small axially directed force [17]. From the flow and density measurements on the MCAS, the force that would applied to the plasma magnet was $0.15 – 0.25$ N. In other words the plasma magnet was able to deflect a plasma wind on the order of what will be desired in space without loss of equilibrium or disconnect from the RMF antenna fields. The effect of this force was observed in a small displacement of the plasmoid upward. This deflection must occur since it is the field tension introduced by the bending of the RMF field that a restoring force can be imparted

32

by the RMF coils as they take up the force delivered by the MCAS. The displacement can be seen in Fig. 11 by observing the relative position of the plasma torus with respect to the Langmuir probe in the right foreground, which was positioned in the equatorial plane of the vacuum chamber. The internal magnetic probe port (back left) was positioned 2 cm above this plane, and can be seen to pass closer to the equatorial plane of the plasma magnet.

Electron Temperature and Density from Double Langmuir Probe
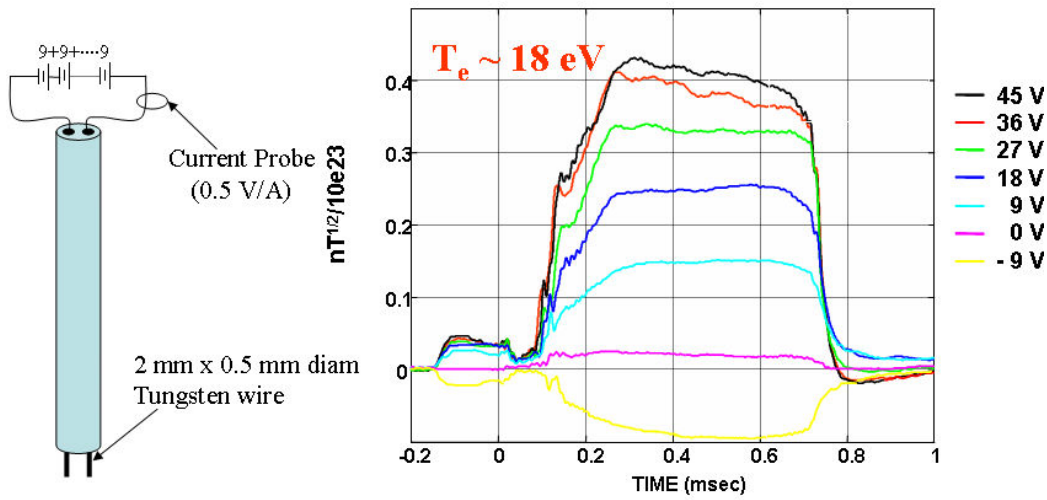
Probe current for symmetric double probe:

$$I = i_+ \tanh\left(\frac{eV_B}{kT_e}\right), \quad \text{where} \quad i_+ = \frac{1}{2}nA_p\left(\frac{k(T_e + T_i)}{M_i}\right)^{\frac{1}{2}}$$

Figure 14

The plasma temperature and density profiles were obtained with a double Langmuir probe. A schematic of the probe and the data from as series of discharges in Argon is shown in Fig. 14. Given the relatively high temperature of the plasma, it is not surprising that it is fully ionized. A check on the consistency of the RMF theory can be made from the data taken with the Langmuir probe combined with the internal magnetic field profile. If all of the electrons move synchronously with the rotating magnetic field, the current density should be specified by knowing the electron density profile, i.e. $J_\theta(r) = en(r)\omega r$ [see eq. (3)]. Conversely, by

measuring the axial magnetic field profile as a function of r in the equatorial plane, and applying Amperes law,

$$J_\theta = \frac{1}{\mu_0} \frac{dB_z}{dr} \tag{13}$$

the current profile can be determined. With the current profile determined from the measured B field, one can obtain the fraction of the plasma electron density that is synchronous with the RMF. The plasma
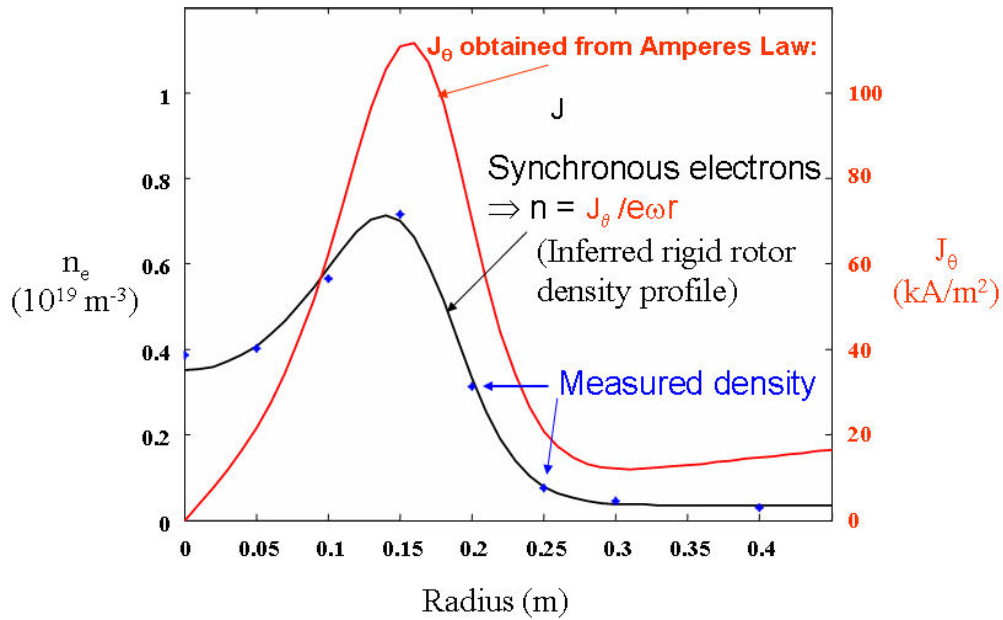

Figure 15. Plasma Magnet Density and Current Profile

must also be in radial pressure balance with surrogate solar wind – the Helmoltz field. There is a unique solution that satisfies both the radial pressure balance constraint as well as the requirement that the electrons rotate rigidly with respect to the rotating field, and it is referred to as a rigid rotor profile, and has the following form:

$$B_z = B_{ez} \tanh K \left(\frac{2r^2}{r_s^2} - 1 \right) \tag{14}$$

The constant K is a fitting parameter determined by axial equilibrium constraints, and in a straight flux conserver, $K \sim R/R_c$, where R is the radius of the plasma magnetic null and R_c is

the chamber radius (remember that the metallic chamber acts as a flux conserver on the timescale of these discharges. One now fits the observed magnetic profile with eq. (14), and solves for the current profile using eq. (13). The result is found in Fig. 15. It can be seen that the observed density profile is very close to what would be expected if all electrons were rotating synchronously with the RMF.
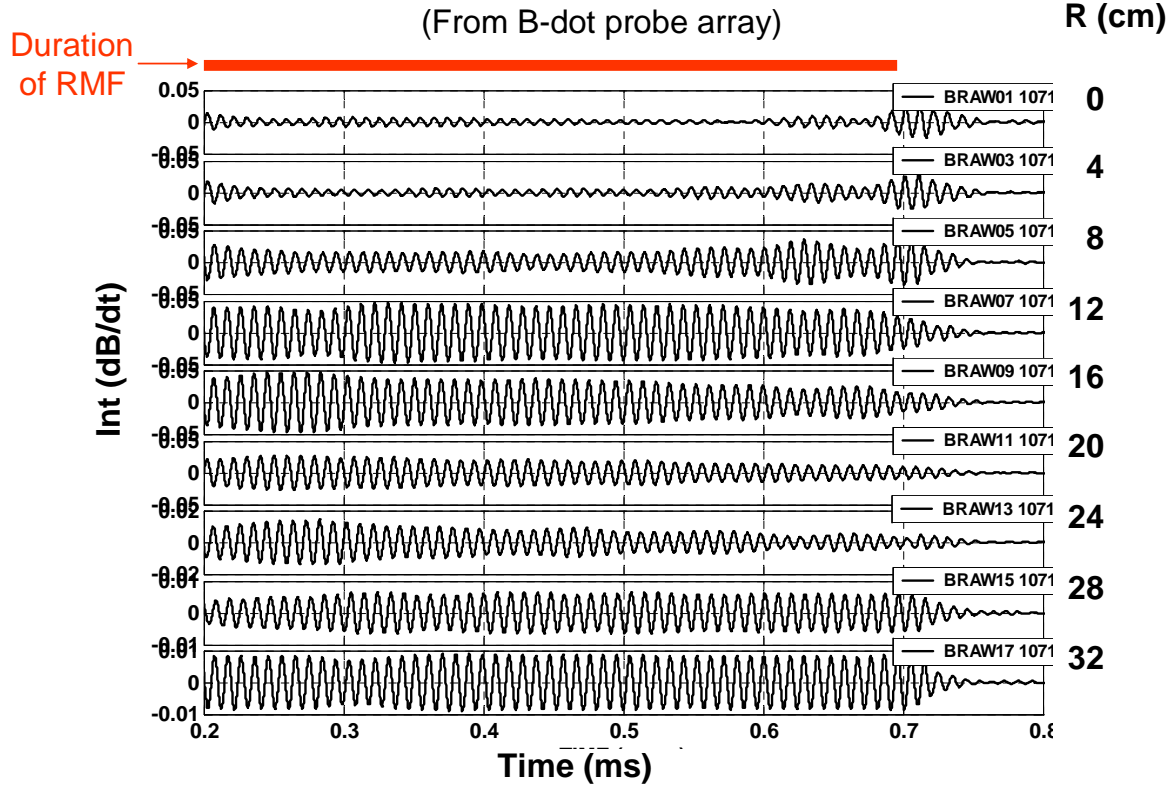

Figure 16. Measurement of the Rotating Magnetic inside the Plasma Magnet as a Function of Radius

The only departure from synchronicity is found near the magnetic axis. This has very little consequence as this region has vanishingly small current density since $j_\theta \to 0$ as $r \to 0$. The lack of drive is consistent with the attenuation of the RMF signal as one approaches $r = 0$. This can be seen in Fig. 16 where the RMF signals from the B probe array are displayed. The amplitude of the RMF changes as one moves from inside to outside of the RMF coils. The presence of the field assures synchronous electron motion. It may appear that all of the current is produced inside the RMF antennas. The plasma equilibrium inside the metal flux conserver forces this to be more the case than not. It should be remembered that the current density

outside the RMF antenna required to achieve a large scale magnetic sail is very small. For the desired 1/r magnetic falloff, the current density should fall off like $1/r^2$ [see eq. (4)]. For the synchronous electrons the current density increases $\sim r$ [(eq. (3) again]. The appropriate plasma density profile will thus fall $\sim 1/r^3$, so that in a linear plot it will always appear as if the plasma or current is found only near the RMF antenna, and in fact most of it is.

.

Future plans for Phase II

The Phase I experiments have demonstrated the ability to drive sufficient current in the plasma magnet to have the resultant dipole field push out well beyond the 10 km scale required for significant interaction with the solar wind. In addition it was demonstrated that a large force imparted on the plasma magnet was reacted back on the RMF antennas with no plasma detachment. The most significant issues left to be tested in validating the plasma sail concept based on the plasma magnet are two-fold. (1) *It must be shown that the plasma magnet can achieve an equilibrium configuration in the presence of a much larger scale solar wind, and that the expected thrust is imparted to the antenna structure.* (2) *It must be demonstrated that the system scales as predicted by code and theory based on the experimental results at small scale.*

The two tasks for the phase II study are thus: (1) **achieve an equilibrium configuration with a much larger solar wind plasma, and measure the thrust delivered to the plasma magnet structure.** (2) **Develop numerical models and analytic analysis sufficient to understand the experimental observations and make scaling predictions that can be tested in further, larger scale tests**. These larger scale tests will of course have to occur in a space-like environment, and would be most likely conducted at an appropriate NASA facility. In this way a logical progression to a space-based demonstration can be pursued in a manner that allows for the modification and optimization of the concept as one progresses to larger scale.

At first it would appear to be an unfeasible task to examine the plasma sail in the laboratory. Fortunately, the expected near linear dependence of dipole field with radius under compression from the solar wind, allows for a scaled experiment that should be very close to producing the results one should obtain in space. With the construction of the proper solar wind source, all of the key dimensionless parameters are unchanged by scaling to a smaller experiment. The only parameter that will not scale is the collisionality of the plasma. As was seen in the phase I demonstration, the current carrying plasma is essentially collisionless even near the source where the plasma density is highest, so this should not be a major concern.

As has been noted, a major attraction of the plasma magnet over other propellantless systems such as the original MagSail or solar sails, is the dynamic expansion of the plasma sail as the spacecraft moves away from the sun and solar wind pressure drops. The converse of course should also be true, and this scaling was taken advantage of in the phase I experiments. It is proposed then to continue to take advantage of this scaling and increase the solar wind pressure until the final plasma sail is on the sub-meter, rather than meter scale. It should be recalled that this is a constant force expansion/contraction - even though the plasma sail is much smaller, the reduction in size is compensated for by the increased solar wind pressure. Thus even in the small-scale laboratory experiments envisioned here, Newton level forces will be delivered to the plasma magnet system, and should thus be straightforward to measure.

The degree that the solar wind pressure must be increased is given by the size of the final standoff distance desired for the laboratory experiment. To obtain the same experimental behavior of the flux surfaces as one would expect to find in the astrophysical context for the plasma magnet, a non-conducting vacuum boundary is desirable. Such a boundary can be provided with the use of large fused silica tubes in place of the usual metal vacuum chamber.
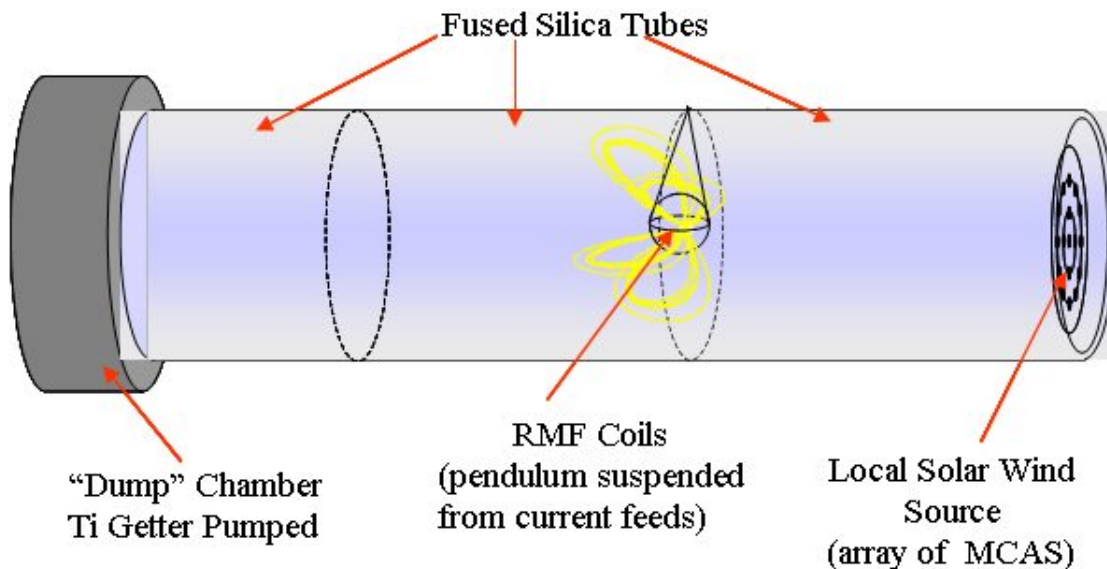

Figure 17. Schematic of proposed facility to demonstrate thrust from a directed plasma flow (LSW) on to a plasma magnetic sail (plasma sail) produced by a rotating magnetic dipole(RMF) field.

Quartz tubes of a meter diameter or more would be prohibitive in cost for a phase II budget, but it is possible to obtain the use of such tubes at the University of Washington. These tubes are remnant from a large fusion experiment [18]. Given the ~ 1 meter diameter of these tubes, the largest stand-off distance should be less than the tube radius and will be assumed to be R_M = 0.3 m. Given the target R_M ~ 30 km desired for the plasma sail in space, the compression ratio in stand-off distance required of the Laboratory Solar Wind source (LSW) over the actual solar wind is ~ 10^5. Since the plasma sail magnetic pressure scales as B^2, and B ~ 1/r under compression, one has that the LSW must produce a pressure that is 10^{10} larger than that of the actual solar wind pressure in order to achieve the desired compression. As large as this factor may seem, it is in fact quite achievable, since the solar wind pressure is a few nPa at earth's orbit. The LSW source must thus achieve a directed plasma pressure of 20 Pa over a radius of ~ 0.4 m. If the plasma velocity is of the same order as the solar wind, then by eq. (8), the power delivered to the laboratory Plasma MagSail is the same as what would be found in the astrophysical context. From eq. (8) for a standoff distance R_M = 10 km, the solar wind power impinging on the plasma sail, P_{sw} ~ 1.4 MW. The LSW must be capable of directed thrust power on this order. This thrust power is beyond the usual plasma thrusters one typically encounters in electric propulsion with the exception of perhaps the MPD thruster. The Isp desired (~ 6,000 s) is also somewhat demanding. A plasma thruster configuration capable of these conditions has been developed and was successfully adapted for this purpose during phase I at much lower power, that thruster being the Magnetized Cascaded Arc Source (MCAS).

The facility that is envisioned to provide a definitive test the plasma sail as a propulsion system is shown in Fig. 17. As can readily be seen, one advantage of using sectioned quartz tubes (section length L = 1.25 m) is that the plasma magnet can be well removed from the solar wind source, with plenty of vacuum space for the downstream wake and magnetotail that may arise from the interaction of the plasma sail and the LSW. This is important since the interaction of the solar wind with the tail could affect the stability of the plasma sail or modify the thrust.

It is also important to maintain a space-like environment inside the vacuum tank as long as possible in order to evaluate the behavior of the plasma sail on timescales much greater than

the ion transit time of the solar wind particles, τ_i, or the formation time of the plasma sail. The time for the establishment of the plasma currents by the RMF was on the order of 0.1 msec in the phase I experiments, and should be comparable here. The directed velocity v_D measured for a D^+ ion emitted by the type of MCAS to be employed here was $v_D = 6 \times 10^4$ m/s. The ion transit time for the ~ 4 m of the quartz interaction chamber will also be < 0.1 msec. It would be desirable to operate the device for a factor of at least 100 times these timescales or ~ 10 msec. The MCAS sources can be operated for up to 100 msec before thermal issues become a problem. In order that the background neutral gas be maintained at high vacuum ($\lambda_{ii} \sim \lambda_{ei} \gg$ L), it is proposed that a plasma burial or "dump" chamber be installed on the downstream end of the experiment. Here, liquid N_2 cooled panels positioned around the circumference, and sprayed with titanium from a titanium evaporator, will pump any plasma or neutral particles that enter the chamber. Using a titanium getter in this way has been shown to trap any particle impinging on the cooled, gettered surface with a sticking probability of near unity. One very nice feature of the MCAS is that the ionization efficiency inside the source is very high and the neutral flow from the source as a fraction of total particle flow is only a few percent.

Laboratory Solar Wind Source

Critical to obtaining an accurate scaling of the solar wind with the plasma sail is the interaction one expects with the solar wind in space. The calculations of this interaction that have been made so far have been made using 3-D Magnetohydrodynamic MHD numerical codes. These codes have been shown to be quite accurate and useful in understanding magnetospheric phenomena. Clearly if one were to start with a magnetosphere of sufficient size and β, the calculations that have been done demonstrate the validity of the concept. The problem comes when the critical phenomena occurs in a regime where the validity of using MHD is a concern. Such is the case of the solar wind interaction with the magnetosphere when the solar wind ion gyroradius, ρ_{sw} in the magnetosphere is greater than the size of the magnetosphere. This is essentially the regime that the plasma sail will be in during start-up. This regime of low interaction persists up to the scale of 20 km where ρ_{sw} would still be ~ 40 km. The behavior of this mixed kinetic - MHD plasma interaction may be quite different than that observed in the numerical MHD calculations. Recent calculations by Khazanov et al. [19]

Contours show the density of the solar wind particles
Source particles are indicated in red.
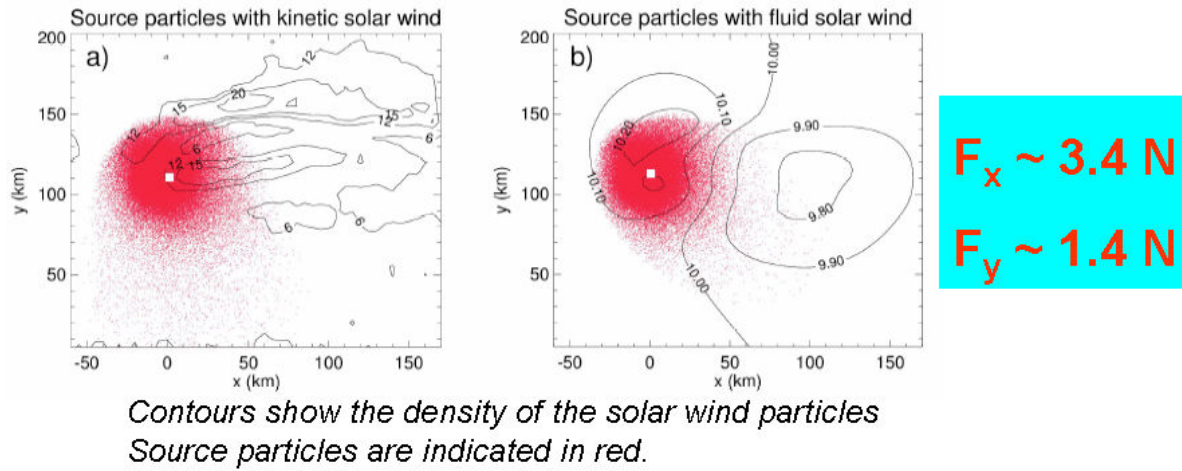
- In the kinetic case (a), the source particles are lost from the bubble in the transverse direction.
- In the fluid case (b), the source particles are lost predominantly in the downstream direction

Figure 18.

showed good agreement with the original work by Winglee et al. in the MHD regime. In the kinetic regime they observed that the partial deflection of the ions reduced the net force and introduced a significant tangential force not seen in the MHD regime. This is important in that the thrust vector is not purely radial making orbit maneuvering with the plasma sail possibly much easier. A plot taken from the Khazanov JPC 2003 pare of the difference in plasma ion motion in these two regimes if found in Fig. 18.

The problems of 3-D MHD simulation are daunting enough, let alone add a component that may only be adequately be described by a full particle in cell calculation. For this reason it is essential that the scaled down laboratory plasma sail be capable of operating in the same regime as the space based plasma sail. In other words, it will be important to obtain conditions where the dimensionless ratio of ρ_{sw}/R_M is of order one. The largest laboratory standoff was assumed to be no greater than 0.3 m. The Deuteron ion gyroradius from the MCAS in a characteristic dipole field of 4 mT is $\rho_{sw} \sim 0.32$ m. Both smaller and larger gyroradii can be obtained by changing the gas used in the solar wind. Hydrogen and Helium have been tested and found to have roughly the same directed velocity as Deuterium. This should allow for a

range of conditions that will allow the kinetic nature of the interaction to be fully explored experimentally.

The plasma source for the solar wind is an array of the magnetized cascaded arc sources (MCAS). Operating in Helium each gun is capable of delivering roughly a solar wind power of $P_{lsw} = 0.5$ N·6x10^4 m/s ~ 30 kW. The devices are fairly easy to construct, and arrays of 8 guns have been operated simultaneously. The plan here is to employ initially ~ 20 devices to provide 0.6 MW of LSW power. If the plasma magnet successfully deflects this power more can be added. In order that the axial magnetic field applied to the MCAS discharge be ignorable on the scale of the interaction region, the field is produced locally by using the return of the discharge current itself to produce the field via a solenoidal winding (See Fig. 13). The scale length of the magnetic disturbance is thus on the order of the MCAS radius, and thus only a few centimeters.

Thrust Measurement

The thrust measurement is obviously a critical measurement for the plasma sail. As such, the system employed to determine the thrust must be incorporated into the design from the outset. The best method for measuring of the directed thrust delivered to the plasma sail, particularly given the high power operation envisioned, is a system of the type used to measure thrust and impulse bit from a high power, pulsed electric thruster. The optical interferometric proximeter system (IPS) developed by Cubbin, Ziemer, Choueiri, and Zahn [20] would be a good choice for this application. Given the very high level of electromagnetic interference from the plasma sources and RMF coils, let alone the magnetic coupling from the plasma sail itself to surrounding metal structures, make it probably the only method for accurately determining the thrust. The principle involved is very simple, and the implementation is reasonably straightforward. The measurement sensitivity covers impulses from 100 μN-s to 10 N-s with an accuracy of better than 2%. Given the values for the plasma magnet-LSW interaction, the impulse bit required to be measured, I_{bit} ~ 240 mN-s, which is well within the range of the IPS measurement capabilities.

The IPS is essentially a Michelson interferometer, which can easily detect movement of an object on the order of a fraction of a wavelength of the laser (~10 nm). The impulse from the

LSW sets in motion the RMF coil system, and its subsequent motion derived from the rate at which the interference fringes change give the momentum change of the plasma sail due to the interaction.   One leg of the Michelson references the chamber wall at the end of the experiment, while the other leg is retro-reflected off the RMF structure. Any relative motion between these two points is measured by tracking the fringe movement. This is very similar to the normal plasma interferometry that is done to obtain the plasma line density, and should represent no particular problem here. In order to allow for unrestricted motion of the RMF structure the power feeds to the RMF system will be made to have a flexible section included at some point.
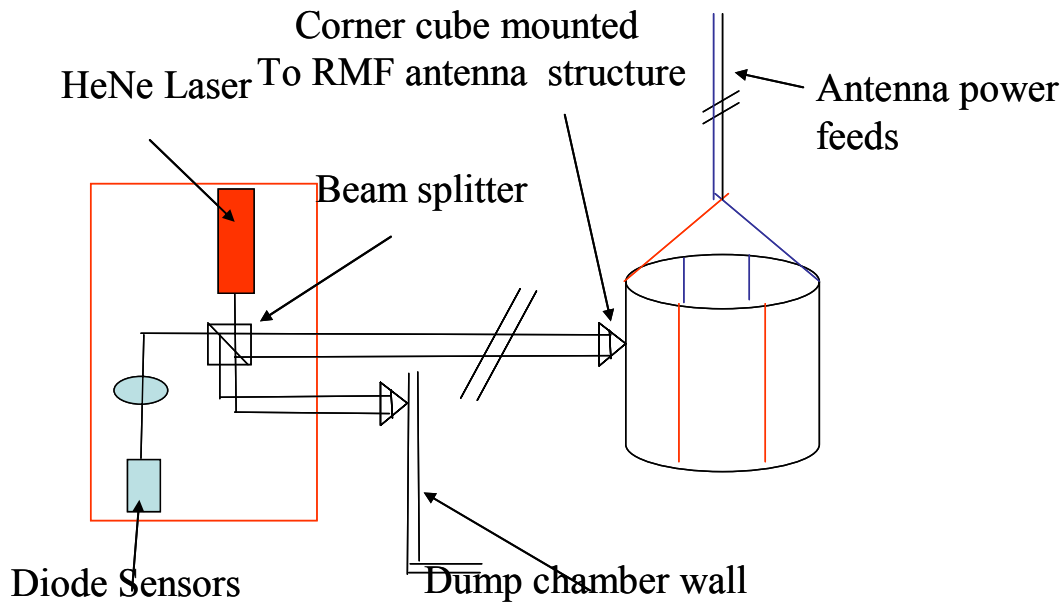

Figure 19. Schematic of the IPS thrust measurement system applied to the plasma magnet

Diagnostic system and code work

In addition to the thrust measurement, it will be important to know as much about the physical behavior of the solar wind plasma interaction with the RMF sustained dipole. The measurement of all the basic quantities, B field, plasma density and temperature, etc. will be made throughout the testing. In particular, once the system has been optimized, a complete mapping of the field and plasma around the plasma sail will be made. In addition to this

experimental task, numerical calculations that include the current drive RMF field will also be made. It is felt that this is an essential step to gain a reasonable ability to extrapolate to larger scale tests as well as the full space-based structure. The MHD codes that have been developed for the study of current drive using a rotating magnetic field will be the starting point [14]. As part of the phase II effort, these codes will be modified to study both the inner and outer dipole configuration. These codes have been remarkable in their accurate prediction of the plasma flows and penetration behavior of the RMF in the experiments. The codes will be benchmarked to the results of the phase II study. A careful comparison of the these code results will then be made with existing predictions based on the Winglee and Khazanov calculations in order to understand the differences if any.

Concluding Remarks

It must be reiterated that the plasma magnet, employed as the source and driver of a large scale plasma sail, has the potential to revolutionize in-space transportation. In particular, it has the possibility of generating propulsive power that far surpasses what is planned for the next generation of space missions, including manned space flight. The chart of various plasma propulsion devices shown in Fig. 20 needs to be log-log in order to put the plasma magnet on the same plot. Only nuclear fusion can span the range of capabilities that the plasma magnet promises, and as difficult as the plasma physics may be in understanding how the plasma magnet will behave on the intended scale, the implementation is orders of magnitude simpler than any nuclear based propulsion system would be.

Comparison of Propulsion Systems

A Plasma Magnetic Sail (PMS) based on the plasma magnet.

Power and exhaust velocity sufficient for rapid manned outer planetary missions
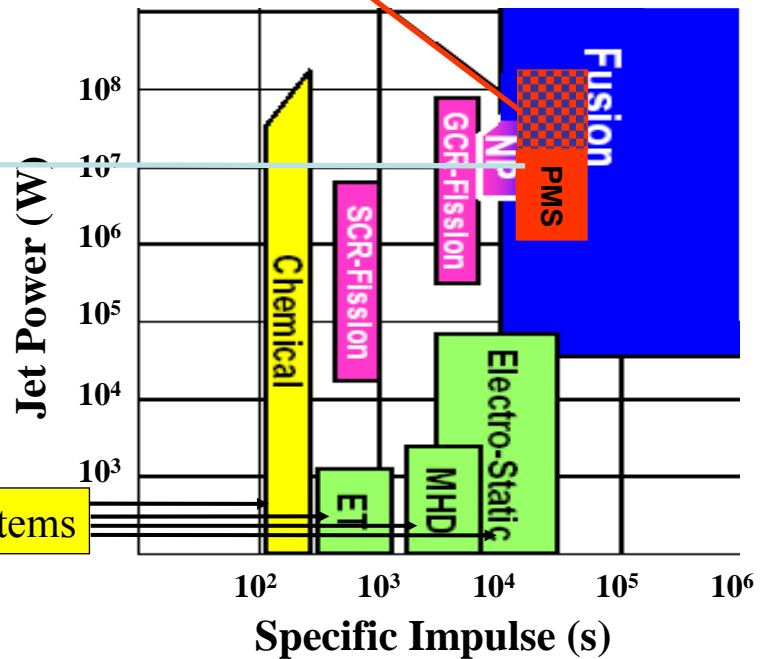
Current propulsion systems

Figure 20.

The great promise of the plasma sail was recognized with the introduction of the M2P2 concept, and the development path was, in the authors view, put on a track that was far to rapid to develop a sufficient understanding of the underlying physics to make the transition from concept to actuality. Even with a firm understanding of the magnetospheric physics, the transition from a laboratory experiment to demonstration was never clearly delineated. Too much was unknown.

The huge advantage of the plasma magnet approach is the great amount of research that has been conducted on the formation, scaling, and high β nature of the plasma in the laboratory. In addition, there is a solid understanding of the current generation physics. With the results from the phase I testing, the appropriate high β, high current plasma has been created and

documented. This of course does not mean that it is time to launch. A directed and orderly approach is still necessary to make sure that there is a successful transition to the larger scale. Along the way, a deeper understanding of the relevant physics can take place. This device is unlike any conventional thruster. It is not enough to know the near field behavior, or for that matter, the far field behavior. It requires an understanding of both. That was not allowed to happen in the previous work on plasma sails for various reasons. Let us hope that this disconnect can be avoided with the plasma magnet. It needs to grow from the promising seed that was revealed in the phase I experiments to the incredible revolutionary propulsion system that it can be if allowed to mature.

References

[1] Zubrin, R.M, "The use of magnetic sails to escape from low Earth orbit", *J. Br. Interplanet. Soc.,* **46** 3 (1993).

[2] Hugrass, W.N., I.R. Jones and M.G.R. Phillips, "An experimental investigation of current production by means of a rotating magnetic field", *J. Plasma Physics* **26**, 465 (1981)

[3] J.T. Slough and K.E. Miller, "Flux generation and sustainment of a Field Reversed Configuration (FRC) with Rotating Magnetic Field (RMF) current drive", *Physics of Plasmas,* **7**, 1495 (2000) [4] Forward, R.L., "Grey solar sails", *J. of Astron. Sciences*, **38** 161 (1990).

[5] R.M. Zubrin and D.G. Andrews, "Magnetic Sails and Interplanetary Travel", *Journal of Spacecraft,* **28** 197 (1991).

[6] R.M. Winglee, J. Slough, T. Ziemba, and A. Goodson, "Mini-magnetospheric plasma propulsion: Tapping the energy of the solar wind for spacecraft propulsion", *J. Geophys. Res.,* **105** 21067 (1999).

[7] R.M. Winglee, .J.T. Slough, K.T. Ziemba, and A. Goodson, "Mini-magnetospheric plasma propulsion: High speed propulsion sailing the solar wind", *Space Technology and Applications*

[8]   John Slough, "High Beta Plasma for Inflation of a Dipolar Magnetic Field as a Magnetic Sail", *Proceedings of the IEPC Conference*, Oct. 14-19, 2001, Pasedena CA.

[9] J.T. Slough and S.P. Andreason, "High field RMF FRC experiments on STX-HF", Submitted to *Phys. Rev. Lett*. (2003).

[10] J.T. Slough and K.E. Miller, "Enhanced Confinement and Stability of a Field Reversed Configuration with Rotating Magnetic Field current drive", *Phys. Rev. Lett*. **85** 1444 (2000).

[11] Hugrass, W.N., I.R. Jones and M.G.R. Phillips, "An experimental investigation of current production by means of a rotating magnetic field", *J. Plasma Physics* **26**, 465 (1981)

[12] S.I. Krasheninnokov, P.J. Catto, R.D. Hazeltine, "Magnetic Dipole Equilibrium Solution at Finite Plasma Pressure", *Physical Review Letters*, **82** 2689 (1999).

[13] D.T. Gernier, J. Kesner, and M.E. Mauel, "Magnetohydrodynamic stability in a levitated dipole", *Physics of Plasmas*, 6 3431 (1999).

[14] R.D. Milroy, "A magnetohydrodynamic model of rotating magnetic field current drive in a field-reversed configuration", *Physics of Plasmas*, **7** 4135 (2000).

[15] J.T. Slough, K.E. Miller, D.E. Lotz, and M.R. Kostora, "Multi-megawatt RF Source for Rotating Magnetic Field Experiments", *Review of Scientific Instruments,* Aug. 2000.

[16] G. Fiksel, et. al, "High current plasma electron emitter", Plasma Sources Sci. Technol. **5**, 78 (1996).

[17] D.J. Rej et al., *"Experimental studies of field-reversed configuration translation",* Phys. Fluids **29**, 852 (1986).

[18] J.T. Slough et al., "Confinement and Stability of Plasmas in a Field Reversed Configuration", *Physical Review Letters*" **69** 2212 (1992).

[19] G. Khazanov et al. "Fundamentals of the plasma sail concept: MHD and kinetic studies", AIAA Joint Propulsion Conference, Huntsville Al., 2003.

[20] E.A. Cubbin, J.K. Ziemer, E.Y. Choueiri, and R.G. Jahn, "Pulsed thrust measurements using laser interferometry", Rev. Sci. Instruments, **68** 2339 (1997).